Journal of Catalysis **208,** 229–237 (2002)
doi:10.1006/jcat.2002.3566, available online at http://www.idealibrary.com on IDEAL®

Interfacial Properties of an Ir/TiO_2 System and Their Relevance in Crotonaldehyde Hydrogenation

P. Reyes,* M. C. Aguirre,* I. Melián-Cabrera,† M. López Granados,† and J. L. G. Fierro†,[1]

*Facultad de Ciencias Químicas, Universidad de Concepción, Casilla 160-C, Concepción, Chile; and †Instituto de Catálisis y Petroleoquímica, CSIC, Campus UAM, Cantoblanco, 28049 Madrid, Spain

Received November 21, 2001; revised February 15, 2002; accepted February 19, 2002

Titania-supported iridium catalysts were prereduced in a hydrogen flow at 473 K (LT) and 723 K (HT). Metal particle sizes determined by H_2 chemisorption and by direct observation of metal particles by transmission electron microscopy were quite similar for LT treatment, and close to 3.0 nm. For the HT case, a large difference in particle size between both techniques is obtained, as a consequence of the H_2 chemisorption suppression (SMSI effect). Photoelectron spectra revealed that iridium is in different oxidation states, with a contribution of 19% $Ir^{\delta+}$ and 81% Ir° species for the LT sample and only a slight increase in $Ir^{\delta+}$ species (26%) for the HT catalyst. Further insights into the surface structures developed by LT and HT treatments were derived from the catalytic performance in the vapor-phase hydrogenation of crotonaldehyde. Activity, expressed as turnover frequency, was more than one order of magnitude higher for the HT catalyst than for its LT counterpart. The interfacial metal–TiO_x moieties, created upon reduction treatment, appeared to be responsible for the increase in activity and in selectivity to crotyl alcohol, via the formation of a [–C=O... surface] σ-bonded complex (detected by *in situ* DRIFTS as a band at 1650 cm^{-1}) stabilized at the metal–TiO_x interface. HT treatment enhances the metal–TiO_x contact, which results in an improvement in catalyst performance. The catalysts deactivate slowly with the time of reaction. Two reasons are advanced to explain the catalyst deactivation: (i) the formation of a strongly chemisorbed asymmetric carboxylate (band at 1740 cm^{-1}); and (ii) the formation of heavy products with conjugated C=O and C=C bonds (band at 1720 cm^{-1}). Both complexes are formed at the expense of the σ-complex and progressively block the active sites responsible for crotonaldehyde hydrogenation. © 2002 Elsevier Science (USA)

Key Words: **iridium; titania; crotonaldehyde; hydrogenation; XPS; DRIFTS; surface analysis.**

---

1. INTRODUCTION

The production of fine chemicals and chemical intermediates routinely involves the selective catalytic hydrogenation of certain chemical bonds to obtain the desired products. One kind of reaction important to fine chemicals is the hydrogenation of α,β-unsaturated aldehydes. These reactions lead to two primary reaction products: the saturated aldehyde and the unsaturated alcohol (see Fig. 1). For small molecules like acrolein and crotonaldehyde the reaction to the saturated aldehydes is favored both by kinetics and by thermodynamics considerations (1–3), while for larger α,β-unsaturated aldehydes, steric restrictions imposed by the substituents on the C=C double bond might influence the product selectivity.

In the presence of most of the conventional group VIII metal hydrogenation catalysts, α,β-unsaturated aldehydes are hydrogenated predominantly to saturated aldehydes by reduction of the C=C group or to saturated alcohols by reduction of both C=C and CHO groups. Therefore, it is desirable to find catalysts which may control the intramolecular selectivity by preferentially hydrogenation of the C=O group while keeping the olefinic double bond intact (Fig. 1, reaction 1 vs 2). Additionally, in order to prevent consecutive hydrogenation to the saturated alcohol (reactions 3 and 4) and the isomerization of the allylic alcohol (reaction 5), the catalyst has to suppress these reaction pathways. Different metals and supports have been used to study the selective hydrogenation of these kinds of unsaturated compounds. Thus, metals such as Co, Pt, Ru, Rh, Os, and Ir have been assayed, showing great differences in activity and selectivity. To improve selectivity to the unsaturated alcohol, metal-supported catalysts have been modified in different ways: by alloying (1, 2), by adding promoters (3, 4), by using strong interactive support (5–8), and by inducing electronic effects and providing appropriate morphologies in the active sites (9, 10). Despite the number of investigations carried out in this field, there is no agreement as to which effect may have a more significant impact on selectivity toward the unsaturated alcohol, because usually two or more effects are acting simultaneously.

Particularly important is the catalytic behavior exhibited by catalysts supported on reducible oxides, which is responsible for the strong metal support interaction (SMSI) effect. Dandekar and Vannice (11) reported significant differences in both activity and selectivity to crotyl alcohol during hydrogenation of crotonaldehyde on Pt-supported catalysts.

---

[1] To whom correspondence should be addressed. Fax: +34-91-585-4760. E-mail: jlgfierro@icp.csic.es.

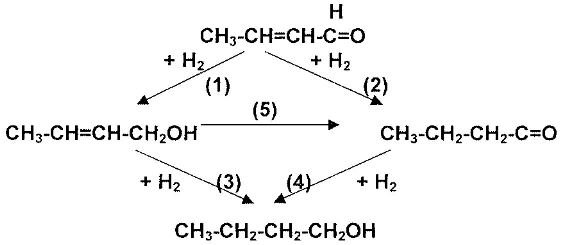

FIG. 1. Reaction network for crotanaldehyde hydrogenation.

In fact, in catalysts in which little or no metal-support interactions should exist, specific activities show similar values. Conversely, Pt/TiO_2 (HT) catalysts, which exhibit the SMSI effect, show much higher values. One of the characteristics of this state is a decrease in H_2 chemisorption capacity produced by physical blockage of the metal surface caused by the migration of TiO_x species during the HT step (12–14).

Even more critical than the differences in activity is the change in selectivity. Thus, the selectivity to crotyl alcohol increases from zero over Pt/SiO_2 and $Pt/\eta\text{-}Al_2O_3$ to 37% over Pt/TiO_2. In all of these samples, the metal was highly dispersed. If the reaction is performed on poorly dispersed catalysts, selectivity to the unsaturated alcohol may reach higher values (8, 15).

Accordingly, this work was undertaken with the aim of modifying the interface between iridium particles and titania substrate by reduction in hydrogen at low (LT) and high (HT) temperatures, which results in different activity and selectivity patterns during the hydrogenation of crotonaldehyde. For this purpose, the surface properties of the catalyst, subjected to two different thermal treatments, were evaluated by H_2 chemisorption, TEM, XPS and *in situ* diffuse reflectance FT-IR spectroscopy. This latter technique provided useful information dealing with possible reaction intermediates and catalyst deactivation in the hydrogenation of crotonaldehyde.

2. EXPERIMENTAL

An iridium–titania catalyst was prepared by impregnation of a TiO_2 (P25-Degussa, $S_{BET} = 72\ m^2/g$) at 298 K with an appropriate amount of aqueous solution of H_2IrCl_6 to get 0.5 wt% of the metal. Then, the sample was dried at 383 K for 24 h and finally calcined at 673 K for 4 h. For the sake of simplicity the sample is referred to hereafter as Ir/TiO_2. Prior to characterization or catalytic use the catalyst was reduced *in situ* in flowing H_2 at 473 (LT) or 723 K (HT) for 2 h.

Hydrogen chemisorption at 298 K was carried out in a volumetric system to evaluate the H_2 uptake. These H_2 uptakes were then used to estimate the Ir dispersion. A surface stoichiometry of $H:Ir = 1:1$ was assumed in all calculations. Before the chemisorption experiments, the sample was reduced *in situ* at LT and HT conditions and then outgassed for 4 h at 773 K.

X-ray diffraction was carried out in Rigaku diffractometer, using a filter of Ni and Cu $K\alpha$ radiation (40 kV and 20 mA). Prior to the experiments, the samples were reduced at 473 and 723 K. The samples were scanned at a rate of 3°/min over a Bragg's angle range of 3–120°. Transmission electron microscopy (TEM) was used for direct observation of supported iridium particles. These experiments were performed in a JEOL JEM-1200 EX-II System. The samples were prepared by the extractive replica procedure.

Diffuse-reflectance infrared spectra (DRIFTS) were collected on a Nicolet-510 FT-IR spectrometer working at a resolution of 4 cm^{-1} (256 scans) using a Harrick HVC-DRP environmentally controlled cell. About 50 mg of the powdered sample was packed in a sample holder and different gases were passed through the sample. First, the sample was reduced in 50 ml/min of pure H_2 at 473 (LT) or 723 K (HT) for 2 h (heating rate 5 K/min). Then it was cooled in H_2 at 373 K. Subsequently, He flow was switched to 50 ml/min and the DRIFT spectrum of the sample was recorded and taken as background. All further recorded spectra were referenced to this background. Then the flow was switched to a reaction mixture, and DRIFT spectra of the sample under the reaction conditions and after different amounts of time onstream were recorded. The reaction mixture was obtained by bubbling H_2 through a saturator containing crotonaldehyde and maintained in an ice bath at 273 K. A number of spectra were recorded after different amounts of time under the reaction conditions. It must be said that recording 256 scans takes ca. 3.5 min; therefore the spectrum is the average of former scans during such a recording time. After some time onstream, the reaction mixture was switched again and He was flowed through the sample. Several spectra were then collected at different times and temperatures, while keeping the sample under a He flow. The high noise detected in the lower wavenumbers of the spectra is a consequence of the strong absorption of the support in this region.

Photoelectron spectra (XPS) were recorded using an Escalab 200R spectrometer provided with a hemispherical electron analyzer, operated in a constant pass energy mode, and a Mg $K\alpha$ X-ray radiation source ($h\nu = 1253.6$ eV). Prior to analysis the samples were reduced in the pretreatment chamber of the spectrometer at 473 and 723 K for 1 h. After this treatment, samples were outgassed until 10^{-6} mbar and then introduced into the analysis chamber. A base pressure of 2×10^{-9} mbar was maintained during data acquisition. The spectral regions of C 1s, Ti 2p, and Ir 4f levels were recorded under high-resolution conditions and averaged for a number of scans in order to obtain good signal-to-noise ratios. The spectra obtained, once the background was removed, were fitted to Lorentzian and Gaussian lines to obtain the number of components, peak position, and their areas. The adventitious C 1s line at 284.9 eV was used as an internal standard. The surface Ir/Ti ratios were estimated from the integrated intensities of Ir (4f) and Ti (2p) lines corrected by the atomic sensitivity factors (16).

Catalytic experiments were carried out in a pulse reactor connected online to a GC. This procedure was chosen because steady-state measurements could not be reached due to strong catalyst deactivation. This deactivation process has been observed in other catalysts, as has been well documented (17). In each experiment 50 mg of catalyst was reduced *in situ* in flowing hydrogen (20 ml/min) in a programmed mode at 10 K/min up to 473 (LT) or 723 K (HT) for 2 h. Then, the sample was cooled to the reaction temperature (323, 343, and 373 K). The catalytic activity was measured by injecting 1.0 μl of the organic reactant. Blank experiments showed no catalytic activity due to the support in these conditions.

3. RESULTS AND DISCUSSION

The metal particle sizes obtained from TEM and the H/Ir atomic ratios are given in Table 1. The H/Ir value is much higher (ca. 10 times) for the catalyst reduced at lower temperature (LT), which indicates a higher metal exposure of LT catalyst. Such a difference is not related to changes in metal dispersion, as is shown by TEM results. The particle size values of the LT catalyst are close to those previously reported for other Ir/TiO$_2$ catalysts prepared under comparable conditions (18). However, a slight but reliable difference is observed between both values, probably due to extra H$_2$ consumption and maybe ascribed to a H$_2$ spillover effect at the chemisorption temperature. TEM analysis revealed only a slight increase in the particle size with the reduction temperature. This apparent discrepancy between chemisorption and TEM data is explained on the basis of the significant decrease in the hydrogen uptake observed in the catalyst reduced at higher temperature (HT). This fact, first identified by Tauster *et al.* (19) is a distinctive feature of the so-called SMSI catalysts. Nowadays, it is well established that chemisorption suppression after HT reduction is a common characteristic of all group VIII metal-supported catalysts on TiO$_2$. The extent of suppression is usually taken as an indication of the development of metal-support interaction and is described as decoration of metal particles by TiO$_x$ species generated upon the reduction process. Obviously, it is expected that this process will occur to a higher extent as temperature increases. The presence of chlorine ions may also produce a slight suppression in the hydrogen uptake. The presence of residual chlorine, reported previously by Bastein *et al.* (20) and Orita *et al.* (21), was found to be responsible for the decrease in CO hydrogenation activity on Rh/TiO$_2$ and was explained in terms of a chloride-assisted TiO$_x$ migration toward metal particle.

TABLE 1

H/Ir Ratios Obtained from H$_2$ Chemisorption, Particle Size Evaluation by TEM, Binding Energies (BE) of Ir 4f$_{7/2}$ Core Electrons, and Ir/Ti Surface Atomic Ratios for a 0.5 wt% Ir/TiO$_2$ Catalyst

Catalyst	H/Ir	D (nm)		Ir 4f$_{7/2}$ BE (eV)	Ir/Ti
		Chem	TEM		
Ir/TiO$_2$-LT	0.570	1.9	2.8	61.0 (81) 62.7 (19)	0.021
Ir/TiO$_2$-HT	0.055	20.0	3.2	60.4 (74) 62.7 (26)	0.020

An X-ray diffraction pattern of the Degussa P25 TiO$_2$ sample used as support showed the characteristic diffraction lines of both rutile and anatase phases. An 85% anatase and 15% rutile has been calculated. This latter phase is the most stable but complete transformation of anatase to rutile takes place at about 1300 K. However, this may occur at lower temperatures in the presence of foreign elements which can catalyze this transformation (22). The activated catalysts did not show any change in support crystallinity, in agreement with previous findings which have shown that for M/TiO$_2$ catalysts a minimum of 2 wt% metal is required to enhance the anatase-to-rutile transformation (22).

The chemical state of iridium at the catalyst surface was determined by photoelectron spectroscopy. For the Ir/TiO$_2$ (LT) sample, the binding energy for the most intense Ir 4f$_{7/2}$ level was found at 61.0 eV for the major component (Ir$^{\circ}$) and at 62.7 eV for the less intense component (Ir$^{\delta+}$) (23) (Table 1). A detectable increase in the proportion of Ir$^{\delta+}$/Ir for the HT treatment together with a slight decrease in the lower binding energy component of the Ir 4f$_{7/2}$ peak was found. Figures 2A and 2B display the Ir 4f core-level spectra for the Ir/TiO$_2$ (LT) and Ir/TiO$_2$ (HT) samples, respectively. As can be seen in Fig. 2, there is overlapping of the strong Ti 3s peak with the Ir 4f doublet. Fortunately, the whole spectrum was accurately decomposed into five lines: two for the Ir 4f$_{7/2}$, another two for the Ir 4f$_{5/2}$, and one for the Ti 3s level. At low temperature, the small metal particles are in intimate contact with the TiO$_2$, making it possible to produce electronic transfer between the support and the metal and generating Ir$^{\delta+}$ species. Additionally, a decrease in the Ir/Ti atomic ratio as reduction temperature increases may be expected due to a migration of TiO$_x$ entities on the surface of the metal crystals producing a decoration of the metallic particles. However, no changes were detected in Ir/Ti ratios (Table 1). This may be understood by considering that the XPS signal averages the contribution of several layers of atoms, including atoms below the metal surface and support atoms. Although the photoelectron process is produced to a depth on the order of several tens of microns, only those photoelectrons produced until depths of approximately 5 nm are reached may be ejected without losing kinetic energy through inelastic scattering processes.

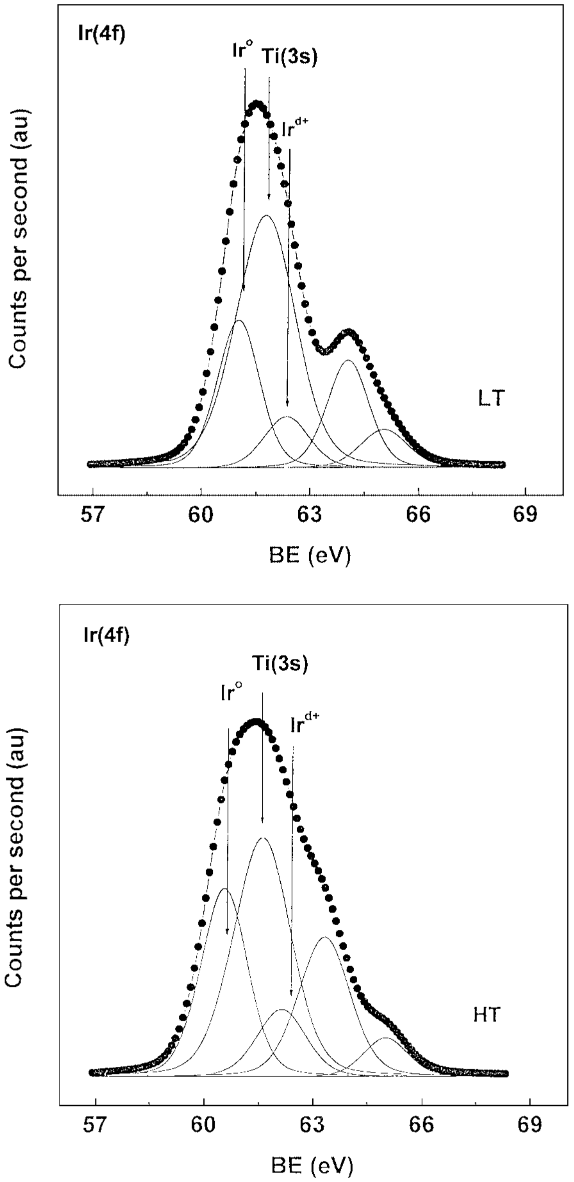

FIG. 2. Ir $4f_{7/2}$ core levels for reduced Ir/TiO$_2$ catalysts at low (LT) and high (HT) temperatures.

Similar arguments may be given to account for the Ir$^{\delta+}$/Ir° ratio. The presence of Ir$^{\delta+}$ species may account for the increase in the selectivity to crotyl alcohol, discussed below.

Hydrogenation of crotonaldehyde was carried out in a pulse reactor at different temperatures, in the range 323–373 K. This alternative allows the initial catalytic activity to be studied without much interference to the deactivation processes. The obtained products were mainly crotylalcohol (CROL), butyraldehyde (BUHO), butylalcohol (BUOH), CO, and products of hydrogenolysis and polymerization. Table 2 summarizes the activity and selectivity of the prepared Ir/TiO$_2$catalysts at the last pulse, whereas Fig. 3A shows the evolution of the conversion level and the

TABLE 2

Catalytic Activity, TOF (s^{-1}), and Selectivity to Crotylalcohol (CROL), Butyraldehyde (BUHO), and Butylalcohol (BUOH) during Crotonaldehyde Hydrogenation at Different Temperatures (Last Pulse) on a 0.5 wt% Ir/TiO$_2$ Catalyst

Catalyst	Temp. (K)	Activity (μmol/s g_{cat}^{-1})	TOF (s^{-1})	Selectivity (mol%) CROL	BUHO	BUOH
Ir/TiO$_2$-LT	323	0.121	0.008	32	67	1
	343	0.242	0.016	21	77	2
	373	0.604	0.041	11	84	5
Ir/TiO$_2$-HT	323	0.242	0.168	34	65	1
	343	0.483	0.337	28	64	8
	373	1.812	1.260	13	60	27

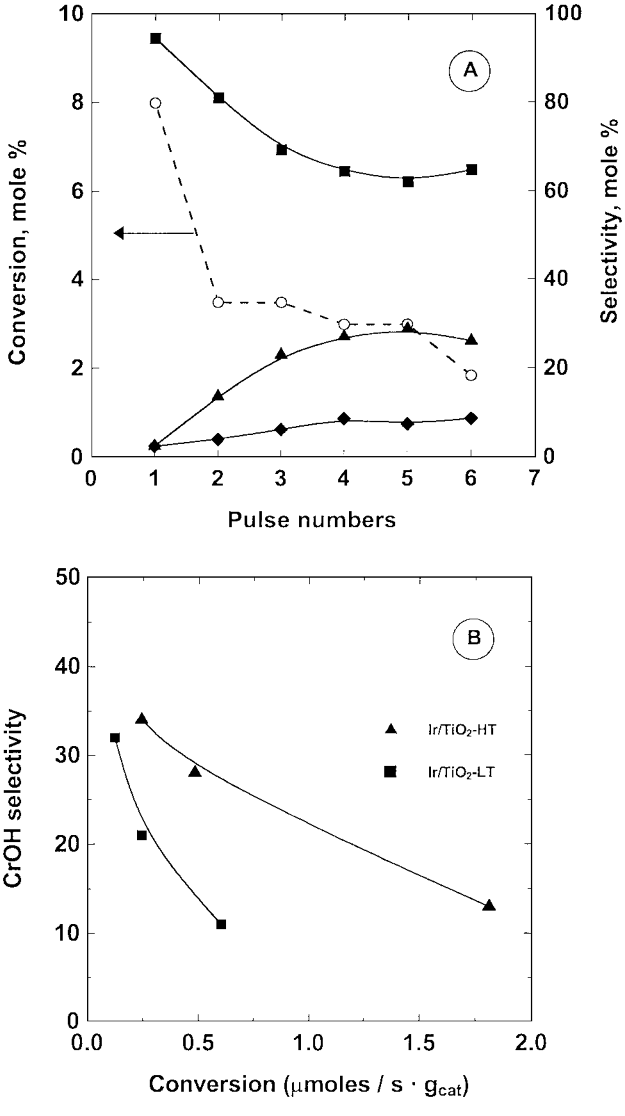

FIG. 3. (A) Product distribution (mole) vs pulse numbers in Ir/TiO$_2$-HT at 343 K: ▲, CROL; ■, BUHO; and ◆, BUOH. (B) Selectivity to CROH against catalyst activity for both LT and HT treatments.

selectivity to the different products with the number of pulses for the HT sample at 343 K.

A significant drop in conversion as the number of pulses increases is observed. In parallel with this change, an enhancement in selectivity to CROL and a decrease in selectivity to BUHO takes place. The data compiled in Table 2 indicate that activity, expressed as micromoles converted per second per gram of catalyst, is twice that for the HT catalyst compared to its LT counterpart. However, more-significant differences were found in the TOF activity, which reaches values more than 20 times higher for the catalyst reduced at high temperature. In both catalysts, the saturated aldehyde is the main product (selectivity higher than 60%) and the selectivity to the unsaturated alcohol is almost zero. However the selectivity to CROL is substantially improved for the HT case, as indicated in Fig. 3B. The selectivity toward CROH for the same conversion was higher for the HT than for the LT treatment. This indicates that many more sites selective for hydrogenation of the C=O bond are present in the HT state. This behavior may be understood by considering that a higher number of Ir/TiO$_x$ interfacial sites are involved (as indicated by the suppression of H$_2$ uptake shown in the HT sample), in spite of the fact that under these conditions a lower amount of metal surface is exposed to the reactant molecules. As Vannice has pointed out (24a), the creation of these new active sites in the interfacial region may explain not only the change in activity but also the change in selectivity. In fact, these sites involved partially reduced TiO$_x$ moieties (or O-vacancies) which coordinate to the oxygen atom in the C=O group to account for a more selective activation of these organic molecule (8, 24a). However, with respect to the active form involved in selective hydrogenation of the carbonyl group, it has been shown that the production of the allyl alcohol starts only after an induction period (24b). The modification of the catalyst surface by the reaction mixture has been considered responsible for the creation of this *in situ*-created center. In terms of our system, this phenomenon is not observed maybe due to the large deactivation upon crotonaldehyde pulses. Further support for this theory is supplied by the DRIFT experiments presented below.

Figure 4 shows the DRIFT spectra obtained under reaction and after switching to a He flow for Ir/TiO$_2$-HT. Figure 5 displays the result of subtracting the DRIFT spectrum of the sample after 5 min under the reaction mixture from the spectrum of the sample after more than 5 min onstream. On the other hand Fig. 6 shows the result of subtracting the DRIFT spectrum of the sample after 120 min under the reaction mixture from the spectra obtained after different times onstream. These last figures are very helpful for seeing bands appearing and disappearing under reaction from different points of view. Figure 5 gives relevance to the alteration of the band intensity with respect to the fresh state and Fig. 6 gives information from the point of view of the highly deactivated state. At the C–H stretching vibration region, bands at 2965, 2930, 2882, and 2718 cm^{-1} predominate. The 2718-cm^{-1} band is assigned to ν(C–H) of the aldehydic group, which suggests that adsorbate containing an aldehyde functional group is present at the surface of the catalyst. They cannot be assigned either to a reaction intermediate or to gas-phase products since band intensity remains when the reaction mixture is switched to a He flow. They must arise from side products or spectators of the reaction which are strongly chemisorbed at the catalyst surface (their intensity is not much altered after flowing He at 473 K). Their concentration at the catalyst surface increases with time onstream, as can be seen in Fig. 5, which means that the surface is progressively covered by such compounds.

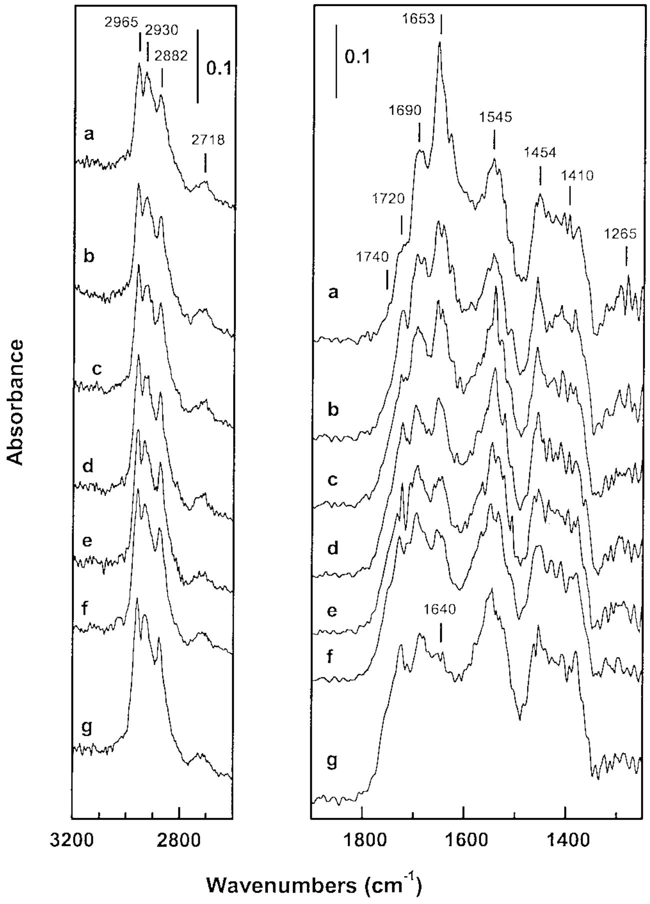

FIG. 4. DRIFT spectra of Ir/TiO$_2$ (HT) during crotonaldehyde hydrogenation at 373 K: (a) after 5 min onstream; (b) at 15 min; (c) at 30 min; (d) at 60 min; (e) at 90 min; (f) at 120 min; and (g) after 5 min under helium flush at 373 K.

Unequivocal assignation of 2965-, 2930-, and 2882-cm^{-1} bands is complicated by the fact that many of the feasible molecules show similar features. They cannot be assigned to C–H vibrations of CH$_x$ groups of weakly adsorbed crotonaldehyde because its bands are placed at quite different

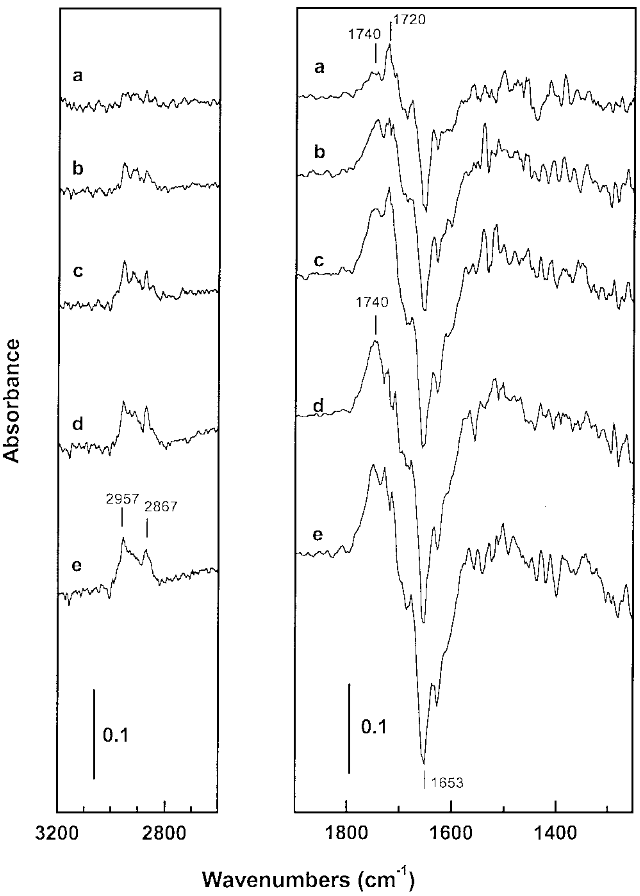

FIG. 5. DRIFT spectra of Ir/TiO_2 (HT) during crotonaldehyde hydrogenation at 373 K after subtraction of 5-min onstream spectrum from (a) 15-, (b) 30-, (c) 60-, (d) 90-, and (e) 120-min spectra.

wavenumbers (25). Olefinic residues can also be discarded because the C=C–H vibrations take place at wavenumbers higher than 3000 cm^{-1}, as pointed out by Sheppard *et al.* (26). It can then be proposed that vibrations at 2965, 2930, and 2882 cm^{-1} arise from saturated alkyl residues strongly adsorbed on metal particles (26). However, the possibility that alkyl chains of other residues strongly chemisorbed at the oxide surface may also contribute to these bands cannot be excluded. Actually Figs. 5 and 6 show different vibration frequencies, which indicates that other residues may be appearing under increasingly higher amounts of time onstream. At lower wavenumbers a feature in the ν(C=O) frequency region is detected (not shown in the figure). This feature did not undergo important changes either under time onstream or after swithing to the He flow, which means that it arises from strongly chemisorbed species. This is attributed to CO adsorbed on Ir arising from the decarbonylation processes of crotonaldehyde. Such CO cannot be discarded as a source of the deactivation (27, 28).

A more complex pattern appears below this region. After 5 min onstream bands at 1720 (m), 1690 (m), 1653 (s), 1545 (s), and 1454 (s) cm^{-1} are clearly detected in Fig. 4a. Wide and featureless bands centered at 1410 (s) and 1265 (s) cm^{-1} are also present. The strong feature at 1653 cm^{-1} is assigned to crotonaldehyde O σ-bonded to coordinatively unsaturated metal cations (Lewis acid sites) in metal oxide surfaces (29). The σ complex is formed between the unshared electron pair on the antibonding n(σ) orbital localized on the oxygen atom of the carbonyl group and the metal cation (30). This adsorption mode has also been described as a donating-on-top η_1 adsorbed species (31, 32). Such interaction results in a 50- to 70-cm^{-1} red-shift of the carbonyl ν(C=O) frequency with respect to gas-phase crotonaldehyde. This band has been observed when α,β-unsaturated aldehydes are chemisorbed on various metals supported on metal oxides (11, 32, 33).

This adsorbate has been said to be the intermediate for the selective reduction of the C=O group in α,β-unsaturated aldehydes (31, 32). Dandekar and Vannice (11) showed a direct relationship between the intensity of this band and the formation of crotyl alcohol from crotonaldehyde and ascribed this band to a different complex: a di-σ

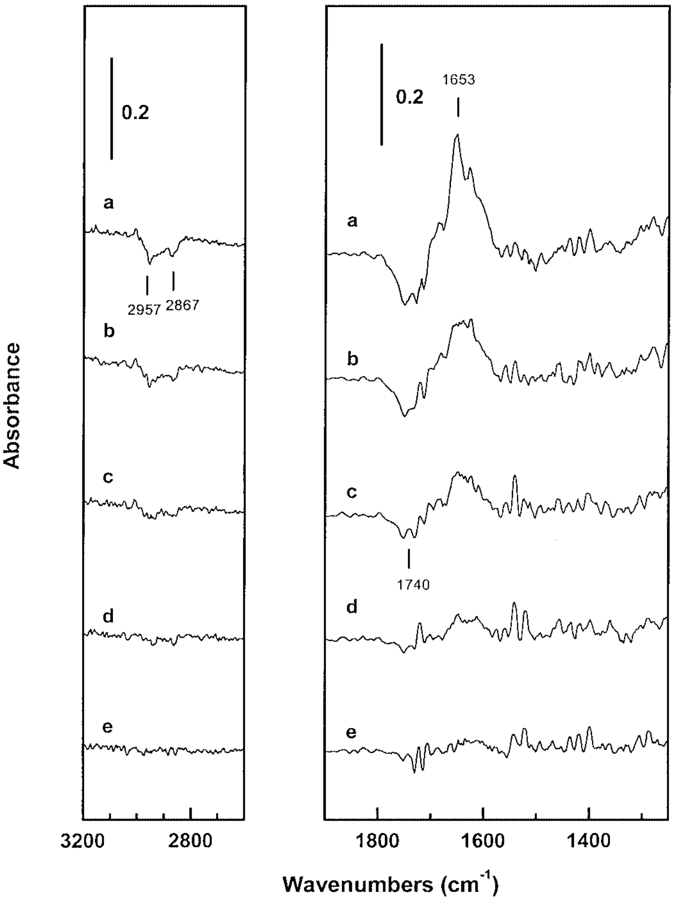

FIG. 6. DRIFT spectra of Ir/TiO_2 (HT) during crotonaldehyde hydrogenation at 373 K after subtraction of 120-min onstream spectrum from (a) 5-, (b) 15-, (c) 30-, (d) 60-, and (e) 90-min spectra.

bond with the C end of the carbonyl group anchored on the metal particle and the O end on the metal cationic sites. In any case the close contact between the hydrogenating site (noble metal particles) and the electrophilic sites (partially reduced metal oxides) is needed for the formation of the selective intermediate species. Some support for this also comes from the slightly higher proportion of $M^{\delta+}$ in this sample (Table 1, Fig. 2), but the 1653-cm^{-1} band can only be explained if TiO_x suboxides are covering the Ir particles. Because the H_2 chemisorption results have clearly indicated that the Ir/TiO_2-HT catalyst is in the SMSI state, this DRIFT band can be considered a probe of the metal covering by the TiO_x species. When the reaction mixture was switched to a He flow, after 5 min of the He flush the C=O feature at 1653 cm^{-1} disappeared, which demonstrates that this species only develops when gas-phase crotonaldehyde is circulating. Thus this disappearance provides additional support for the assumption that the σ complex is an intermediate of the crotyl alcohol formation.

The 1720-cm^{-1} feature does not arise from miscancellation of the crotonaldehyde bands because it is also detected after switching to the He flow, once crotonaldehyde has been removed from the gas phase (Fig. 4g). Its position points to a carbonyl-group-containing compound. It is strongly adsorbed at the surface because the band remains after the He flush at 373 (Fig. 4g) and 474 K (not shown in Fig. 4). Figure 5 indicates that the 1720-cm^{-1} band develops only during the beginning of the reaction since it is visible in Figs. 5a–5c and then its intensity remains rather constant. This band is almost not visible in Fig. 6 because this figure stresses the point of view of the higher deactivated state. According to the literaure, it can be proposed that crotonaldehyde can undergo aldol condensation and oligomerization processes (36, 37) on the catalyst surface, leaving heavy residues containing C=O and C=C functional groups on the surface, which are only removable at high temperatures and which must be taken into account as a source of the deactivation. The C=O groups in this structure are weakly affected by the surface and the vibration frequency approached the frequency (1720 cm^{-1}) of the C=O group of the gas-phase acrolein.

Figures 5 and 6 allow the identification of a band at 1740 cm^{-1} that is barely visible in Fig. 4. Figure 5 shows that the intensity of the 1740-cm^{-1} feature increases with time onstream (see Fig. 5), parallel to the disappearance of the band at 1653 cm^{-1}. Figure 6 confirms this phenomenon but from the point of view of the highest deactivated state: positive intensity of the 1653-cm^{-1} feature indicates that during the lower amount of time onstream such a band was more intense than in the 120-min onstream spectrum. A band at 1653 cm^{-1} has been found when α,β-unsaturated aldehydes are chemisorbed on a metal oxide surface with electron-donor centers (oxygen ions): an asymmetric butanoate chemisorbed on the TiO_2 surface is formed by nucleophilic attack of surface oxygen to the electrophilic C atom of the carbonyl group (29, 30). The blueshift of the ν(C=O) frequency with respect to the gas-phase crotonaldehyde vibration is related to the electron-donor nature of the surface O sites that shortens the C=O bond. It has been reported that the O σ-bonded of C=O group is transformed to an asymmetric surface carboxylate complex when heated or when increasing the aldehyde–metal oxide surface contact time (29, 30). Therefore, it can be proposed that the catalyst deactivation must be related to the transformation of the active intermediate into an inactive and strongly chemisorbed surface asymmetric carboxylate spectator while the catalyst is under the reaction conditions.

H-bonded crotonaldehyde interacting with Brønsted OH sites of TiO_2 support accounts for the 1690-cm^{-1} band: this interaction weakens the carbonyl C=O bond and lowers by 20-30 cm^{-1} the ν(C=O) frequency (25, 30) compared to the gas-phase value. This adsorbed crotonaldehyde species must show another less intense band at ca. 1640 ascribable to the ν(C=C) bond (25) but it is obscured by the strong one at 1653 cm^{-1} (it appears as a shoulder of it) and is only observable when crotonaldehyde is flushed (Fig. 4g). After He switching the 1690-cm^{-1} feature remains, which indicates that this complex is strongly chemisorbed on the support surface and it is not involved in the reaction mechanism. It must be said that a negative peak in the ν(O-H) frequency of Ti–OH surface groups was observed (not shown in Fig. 4). Negative absorption, in this case, means that such OH groups are perturbed by interaction with any of the molecules present under the reaction conditions. Anatase is assumed not to exhibit Brønsted acidity; however weak bases like benzene have been shown to interact with Ti–OH groups of anatase by H-bonds and to shift the stretching modes of the O–H groups to lower frequencies (38). Moreover stronger acid O–H sites can be present at the surface of the TiO_2 since impurities like S (sulfates) and P (phosphates) are present in most commercial Ti oxides (39). Any former phenomena can explain the negative feature but, in any case, these interactions are irrelevant to mechanism clarification since no intensity variations are detected when switching to a He flow: they very likely arise from spectator–OH group interactions.

The 1545- and 1454-cm^{-1} bands can be ascribed to symmetric carboxylate (crotanoates or butanoates) (R–CO_2^- group) (25, 30, 33, 34). It has been suggested that symmetric complexes are related to the lack of crotyl alcohol formation while onstream (33), but considering that the disappearance of the 1653-cm^{-1} band is not related to any change in the carboxylate group frequencies, such a hypothesis can be discarded. Moreover the symmetric carboxylate complex bands develop rapidly and the intensity reached after 5 min onstream remains almost constant under time onstream (see Figs. 5 and 6). They were not removed after switching to a He flow, even after heating under He at

473 K, which indicates that these complexes are strongly chemisorbed and are not involved in the reaction.

Figure 7 shows the DRIFT spectra under reaction conditions and after a He flush of the Ir/TiO_2-LT sample. Figure 8 presents the results of subtracting the DRIFT spectrum of the sample after 5 min under the reaction mixture from the spectra of the sample after more than 5 min onstream. The spectra are much simpler. Negative features (not shown) in the 3800- to 3600-cm^{-1} region and at 2044 cm^{-1} can be assigned to interaction of the spectators with the OH groups. ν(C-H) frequencies were too weak and they could not be detected. The 5-min spectrum is dominated by the band at 1650 cm^{-1}, which vanishes under a He flush, which is ascribable to crotonaldehyde O σ-bonded to coordinatively unsaturated metal cations (Lewis acid sites) in metal oxide. The intensity of this band is lower than that for Ir/TiO_2-HT, which can explain the lower activity and CrOH selectivity of the LT catalyst. Moreover, the weaker intensity of this band can arise from a lower coverage of Ir particles by TiO_x moities with respect to the HT state. Such an effect was clearly detected by H_2 chemisorption and was also suggested in the Ir 4f core-level spectra (Fig. 2). It seems that a DRIFT band at 1650 cm^{-1} is a valuable probe for detecting the coverage of metal particles by TiO_x patches. No other intense bands were detected although featureless and wide low intense bands can be detected at lower wavenumbers.

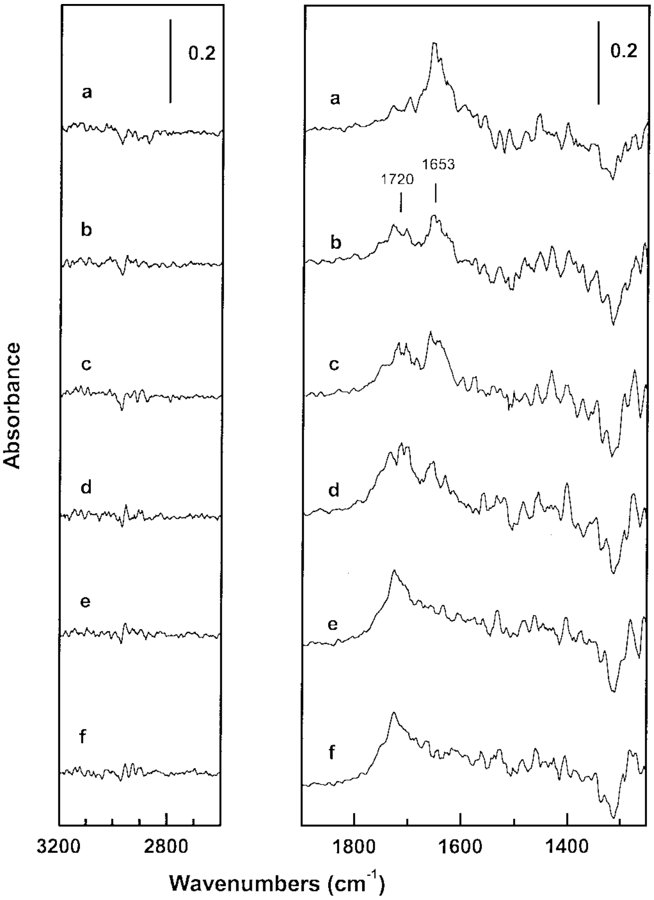

FIG. 7. DRIFT spectra of Ir/TiO_2 (LT) during crotonaldehyde hydrogenation at 373 K: (a) after 5 min onstream; (b) at 15 min; (c) at 30 min; (d) at 90 min; (e) after 15 min under helium flush at 373 K; and (f) after 30 min under helium flush at 373 K.

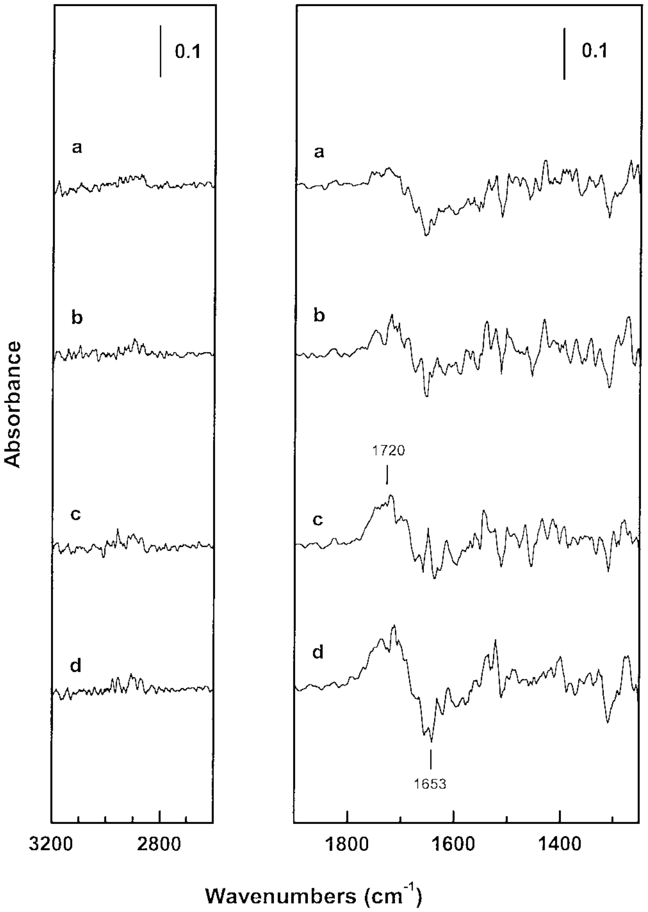

FIG. 8. DRIFT spectra of Ir/TiO_2 (LT) during crotonaldehyde hydrogenation at 373 K after subtraction of 5-min onstream spectrum from (a) 15-, (b) 30-, (c) 60-, and (d) 90-min spectra.

After longer time onstream, the 1650-cm^{-1} band becomes less intense whereas a new wide band at 1720 cm^{-1} predominates. The second band is ascribed above to the formation of heavy products containing C=O and C=C functionalities arising from crotonaldehyde aldol condensation on TiO_2 surface. This wide band seems to display a shoulder at 1740 cm^{-1}. Detection by subtraction (Fig. 8) is not conclusive. This band was assigned to the formation of asymmetric carboxylate as a result of the O lattice nucleophilic attack on the carbonyl group. Figure 8 shows that the intensity of the former band(s) grows whereas the band at 1650 cm^{-1} vanishes, which confirms that these complexes can be involved in deactivation processes in LT catalyst. On the other hand, it must be stressed that bands arising from symmetric carboxylate complexes were not observed in Fig. 6 and therefore they cannot be responsible for deactivation, as has been suggested in previous works.

4. CONCLUSIONS

A titania-supported catalyst exhibits different surface and catalytic properties after reduction at low or high temperatures. High-temperature reduction (HT) induces the decoration of Ir particles generating metal–TiO$_X$ moieties, which appear to be responsible for the increase in the activity of crotonaldehyde hydrogenation and in selectivity to crotyl alcohol. *In situ* DRIFTS studies have shown the formation of a [–C=O… surface] σ-bonded complex, characterized by a band at 1650 cm^{-1}, which became stabilized at the metal–TiO$_x$ interface. HT treatment enhances the metal–TiO$_x$ contact and improves the catalytic properties of the Ir/TiO$_2$ catalyst. The catalytic performance in the vapor-phase hydrogenation of crotonaldehyde showed that turnover frequency was more than one order of magnitude higher for HT catalyst than for its LT counterpart. Deactivation of the catalysts takes place under onstream operation. Two proposals are advanced to explain the catalyst deactivation: (i) the formation of a strongly chemisorbed asymmetric carboxylate (band at 1740 cm^{-1}); and (ii) the formation of heavy products with conjugated C=O and C=C bonds (band at 1720 cm^{-1}). Both complexes are formed at the expenses of the σ-complex and block the active and selective sites.

ACKNOWLEDGMENTS

The authors thank CONICYT (Chile) through FONDECYT Research Grants 1980345 and 2990065 and CSIC-CONICYT bilateral cooperative programme for financial support.

REFERENCES

1. Raab, G. C., and Lercher, J. A., *J. Mol. Catal.* **75**, 7 (1992).
2. Bonnier, J. M., Damori, J. P., and Masson, J., *Appl. Catal* **42**, 285 (1988).
3. Marinelli, T. B. L. W., Nabuurs, S., and Ponec, V., *J. Catal.* **151**, 431 (1995).
4. Sepúlveda-Escribano, A., Coloma, F., and Rodriguez-Reinoso, F., *J. Catal.* **178**, 649 (1998).
5. Galvagno, S., Milone, C., Neri, G., Donato, A., and Pietropaolo, R., *Stud. Surf. Sci. Catal.* **78**, 163 (1993).
6. Yoshitake, H., and Iwasawa, Y., *J. Catal.* **125**, 227 (1990).
7. Coq, B., Kumbhar, P. S., Moreau, C., Moreau, P., and Figueras, F., *J. Phys. Chem.* **98**, 10180 (1994).
8. Vannice, M. A., and Sen, B., *J. Catal.* **115**, 65 (1989).
9. English, M., Jentys, A., and Lercher, J. A., *J. Catal.* **166**, 25 (1997).
10. Galvagno, S., Milone, C., Donato, A., Neri, G., and Pietropaolo, R., *Catal. Lett.* **18**, 211 (1993).
11. Dandekar, A., and Vannice, M. A., *J. Catal.* **183**, 344 (1999).
12. Vannice, M. A., *Catal. Today* **12**, 255 (1992).
13. Haller, G. L., and Resasco, D. E., *Adv. Catal.* **36**, 173 (1989).
14. Munuera, G., González-Elipe, A. R., Espinós, J. P., Conesa, J. C., Soria, J., and Sanz, J., *J. Phys. Chem.* **91**, 6625 (1987).
15. Vannice, M. A., *Top. Catal.* **4**, 241 (1997).
16. Wagner, C. D., Davis, L. E., Zeller, M. V., Taylor, J. A., Raymond, R. H., and Gale, L. H., *Surf. Interface Anal.* **3**, 211 (1981).
17. Raab, G. C., and Lercher, J. A., *Catal. Lett.* **18**, 99 (1993).
18. Reyes, P., Aguirre, M. C., Pecchi, G., and Fierro, J. L. G., *J. Mol. Catal.* **164**, 245 (2000).
19. Tauster, S. J., Fung, S. C., and Garten, R. L., *J. Am. Chem. Soc.* **100**, 170 (1978).
20. Bastein, A. G. T. M., van der Boogert, W. J., van der Lee, G., Luo, H., and Ponec, V., *Appl. Catal.* **29**, 243 (1987).
21. Orita, H., Naito, S., and Tamaru, K., *J. Phys. Chem.* **89**, 3066 (1985).
22. Resasco, D. E., Ph.D. thesis. Yale University, New Haven, Connecticut, 1983.
23. Briggs, D., and Seah, M. P., Eds., "Practical Surface Analysis: Auger and X-Ray Photoelectron Spectroscopy." Wiley, Chichester, 1990.
24. (a) Vannice, M. A., *J. Mol. Catal.* **59**, 165 (1990). (b) Ponec, V., *Appl. Catal. A* **149**, 27 (1997).
25. Rekoske, J. E., and Barteau, M. A., *Langmuir* **15**, 2061 (1999).
26. Sheppard, N., and de la Cruz, C., *Adv. Catal.* **41**, 1 (1996).
27. de la Cruz, C., and Sheppard, N., *J. Chem. Soc. Faraday Trans.* **93**, 3569 (1997).
28. Coloma, F., Coronado, J. M., Rochester, C. H., and Anderson, J. A., *Catal. Lett.* **51**, 155 (1998).
29. Serwicka, M., Black, E. J. B., and Goodenough, J. B., *J. Catal.* **106**, 23 (1997).
30. Popova, G. Ya., Davydov, A. A., Andrushkevich, T. V., and Zakharov, I. I., *Kinet. Catal.* **36**, 125 (1995).
31. Ponec, V., *Appl. Catal.* **149**, 27 (1997).
32. Nishiyama, S., Hara, T., Tsuruya, S., and Masai, M., *J. Phys. Chem.* **103**, 4431 (1999).
33. Bailie, J. E., Rochester, C. H., and Hutchings, G. J., *J. Chem. Soc. Faraday Trans.* **93**, 4389 (1997).
34. Yee, A., Morrison, S. J., and Idriss, H., *J. Catal.* **186**, 279 (1999).
35. Popova, G. Ya., Andrushkevich, T. V., Meshcheryakov, V. D., and Davydov, A. A., *Kinet. Catal.* **31**, 351 (1990).
36. Kubelkova, L., and Trifirò, F., *J. Catal.* **26**, 242 (1972).
37. Luo, S., and Falconer, J. L., *Catal. Lett.* **57**, 89 (1999).
38. Busca, G., Saussey, H., Saur, O., Lavalley, J.-C., and Lorenzelli, V., *Appl. Catal.* **14**, 245 (1985).
39. Hadjivanov, K. I., and Klissurski, D., *Chem. Soc. Rev.* **25**, 61 (1996).